doi.org/10.62683/SINARG2025.139

Research paper

COMPUTATIONAL ANALYSIS OF FREE-EDGE EFFECTS IN COMPOSITE LAMINATES USING ABAQUS

Milica Živković[1], Emilija Jočić[2], Miroslav Marjanović[3]

Abstract

The free-edge effects are related to singular stress states at the interfaces between dissimilar layers in the vicinity of geometrical or mechanical discontinuities within the laminar composite. Stress concentration at free edges can further lead to delamination and a significant drop in stiffness, with fracture occurring at lower loads than expected. The paper deals with the computational (finite element) modeling of free-edge effects in cross-ply composite laminates. For this purpose, Abaqus software package has been used and two solid finite element types have been applied. Free-edge stress field of laminar composites under axial extension has been analyzed. Several numerical examples of cross-ply composites with various stacking sequences have been presented, and the results are compared against the existing analytical solutions based on the improved first-order shear deformation theory. Additionally, a parametric study has been conducted, focusing on the variation of τ_{yz} stresses through free edges as a function of plate thickness.

Key words: *Free-edge stresses, laminate, composite, plate, axial loading*

[1] BSc Civil Eng., Junior Teaching Assistant, University of Belgrade – Faculty of Civil Engineering, Serbia, mizivkovic@grf.bg.ac.rs, 0009-0001-0629-544X
[2] PhD Civil Eng., Assistant Professor, University of Belgrade – Faculty of Civil Engineering, Serbia, edamjanovic@grf.bg.ac.rs, 0000-0001-9099-8983
[3] PhD Civil Eng., Associate Professor, University of Belgrade – Faculty of Civil Engineering, Serbia, mmarjanovic@grf.bg.ac.rs, 0000-0001-9790-912X

1. INTRODUCTION

Because of their exceptional strength, stiffness and corrosion resistance, laminar composites have found an extensive application in construction of mechanical, aerospace, marine and automotive structures, typically demanding high reliability levels. When subjected to tension, they may fail through various scenarios, such as fiber breakage and pull out, matrix yielding and cracking, among others. Their ultimate strength and failure mechanisms depend on geometrical factors and material properties; therefore, a detailed study of their failure behavior is a crucial step towards the safe and reliable structural design [1].

Since the adjacent layers cannot move independently when loaded, normal and shear stress concentrations occur to satisfy the displacement compatibility conditions in the presence of different Poisson's ratios, elastic and shear moduli and thermal expansion coefficients of the adjacent layers. These stress concentrations are pronounced at the free edges of a laminar composite, which can further lead to delamination and a failure at loads significantly below the expected limit level. The stress concentrations decrease with distance from the free edges of the plate, gradually diminishing to negligible values. Their magnitude is also a function of layer orientation, layer thickness, boundary conditions, and loading type, as well. Under axial strain, the stress concentrations at the free edges are generally lower when compared to laminar composites in bending or torsion [2, 3].

Starting from the earliest work on this topic by Pipes and Pagano [4], various numerical and approximate analytical solutions have been derived so far to accurately identify and evaluate interlaminar stresses associated with the free-edge effect. A comprehensive review of different approaches can be found in [5, 6].

Exact analytical solutions for free-edge stress singularities are typically limited to simplified layups and loadings. Becker [7] proposed closed-form solutions using higher-order plate theory for free-edge stresses in cross-ply laminates. Nosier and Bahrami [8] and Nosier and Maleki [9] applied both the improved first-order shear deformation theory (FSDT) and the layerwise theory (LWT) to study free-edge effects in angle-ply and general laminates, incorporating reduced constitutive relations and traction-free boundary conditions. Beside the limited number of analytical solutions, a number of numerical solutions has been derived, such as 3D FEM-based solution by Wang and Crossman [10].

In this paper, the Abaqus [11] software is used to analyse the stress state near the free edges of a layered composite. Abaqus is a software application used for both the modeling and analysis of mechanical components and assemblies (pre-processing) and visualizing the finite element analysis results (post-processing). Abaqus has a large library of finite elements of different types, and two of them have been used for the purpose of this work. Using two different finite element types, interlaminar shear (τ_{yz}) and normal stress (σ_z) distributions are analyzed through the width of a layered composite, in the vicinity of free edges. Different stacking sequences are analyzed. For σ_z, the stress distribution through the plate thickness is also studied for a composite with an conventional cross-ply stacking sequence. Finally, a parametric study is performed to investigate the influence of layer thickness on the through-the-width distribution of the interlaminar shear stress τ_{yz}.

The obtained results are compared with analytical solution based on the first-order shear deformation theory, proving the high accuracy of applied numerical models, and the appropriate conclusions are derived.

2. MODELING OF LAMINAR COMPOSITE USING ABAQUS

For modeling purposes, the rectangular laminated composite plate is first created as a homogenous body (prism). By using a separation tool, several layers of the same height are created within the solid body (part). Therefore, a tie-constraint between the layers have been introduced. The linear elastic orthotropic material is modeled by specifying 9 independent engineering constants: moduli of elasticity E_i, shear moduli G_{ij} and Poisson's ratios ν_{ij}. Appropriate layer orientation is assigned by rotating local coordinate systems of the material within 90° layers. Uniform axial strain is assigned by applying translational displacements along the free edges, $u(a) = \bar{U}$ and $u(0) = -\bar{U}$, in order to achieve the strain of $\varepsilon_x = 10^{-6}$.

For the analysis of free-edge effects, meshing is performed by using two different types of solid finite elements. The **C3D8R** is a general-purpose linear brick element with reduced integration. It has one integration point in the center of the finite element. Nodes are located at the corners, and each node has 3 generalized displacements (24 degrees of freedom in total). The **C3D10** is a quadratic general-purpose tetrahedral element, with nodes in corners and mid points of the edges (see Figure 1). Each node has 3 generalized displacements (30 degrees of freedom in total), while the integration is performed in 4 integration points [12].

Figure 1. C3D8R and C3D10 finite elements in Abaqus, with their respective nodes and integration points (red color)

3. NUMERICAL RESULTS AND DISCUSSION

This section presents the obtained results from the conducted numerical analyses. The calculated free-edge stresses are compared with those obtained analytically [2]. Distibution of stresses is analyzed through the width and through the thickness of the considered plate-like models, with different stacking sequences.

3.1 Considered model geometry

For the analysis, a 4-layers rectangular laminated composite plate with dimensions $a \times 2b$ has been analyzed (Figure 2). Plate length is $a = 10h$, width is $b = 2h$, while layer thickness is $h_k = h/4$, where h is the total plate thickness. Each layer is a unidirectional reinforced composite made of material with the following properties in material coordinates: $E_1 = 137.9$ GPa, $E_2 = E_3 = 14.48$ GPa, $G_{12} = G_{13} = G_{23} = 5.86$ GPa, while $\nu_{12} = \nu_{13} = \nu_{23} = 0.21$. Three stacking sequences have been considered: two symmetric ones, $[0^o/90^o]_s$ and $[90^o/0^o]_s$, as well as the conventional cross-ply $[0^o/90^o/0^o/90^o]$ sequence.

For the through-the-thickness interpolation, three sub-laminate discretizations have been considered, including P=1, P=2 or P=4 sublayers through each material layer, respectively.

This leads to the total of 4, 8 or 16 sublayers through the entire plate thickness. For the in-plane discretization, three mesh densities have been considered, including element sizes of $h/4$ (Mesh 1), $h/8$ (Mesh 2) and $h/16$ (Mesh 3). Table 1 elaborates the number of sublayers in each material layer, for each considered mesh density.

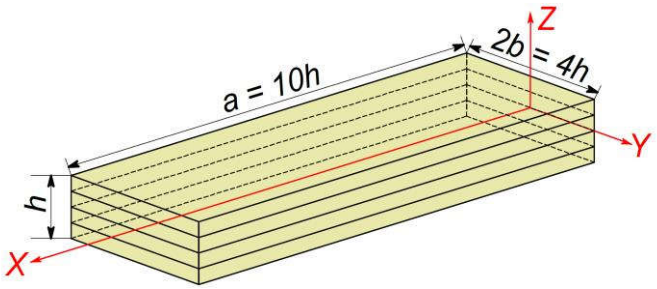

Figure 2. Considered laminated composite plate with four layers

Table 1. Number of sublayers depending on FE dimensions

FE dimension	h_k	$h_k/2$	$h_k/4$
number of sublayers (P)	1	2	4

3.2. Distribution of the interlaminar shear stress τ_{yz}

In Figure 3, the distribution of τ_{yz} through the width of the plate with $[90^o/0^o]_s$ and $[0^o/90^o]_s$ stacking sequences is displayed. Interlaminar shear stress is near zero in the middle and increases toward the free edge where it reaches its maximum values. The displayed results were measured at $z = h_k$ interface. The C3D10 elements (red lines) showed better accuracy against the C3D8R (blue lines) in predicting both the position and the value of the maximum stress, when compared against the analytical solution [2] (black line). As expected, mesh refinement led to the convergence to analytical solution.

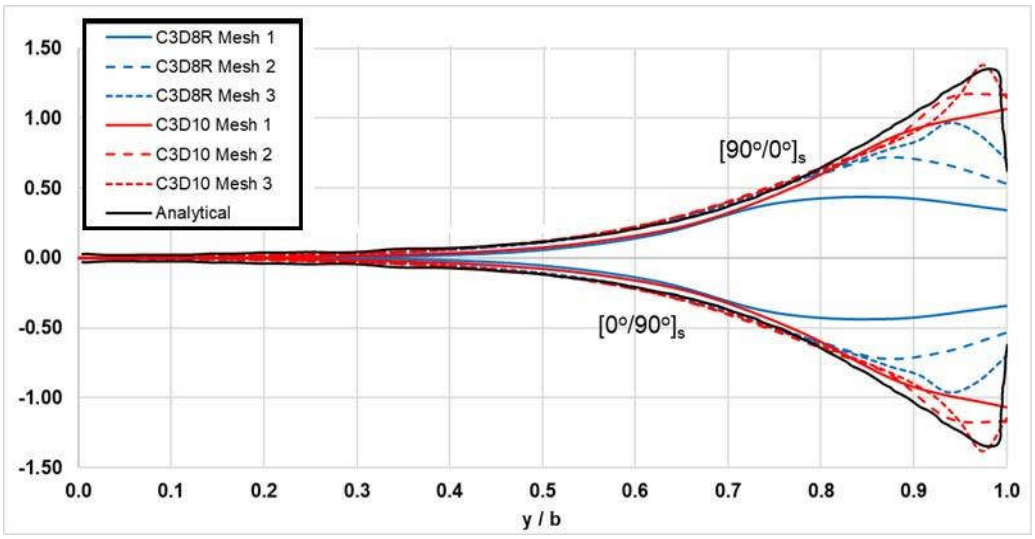

Figure 3. Dimensionless interlaminar shear stress (τ_{yz}/ε_0)×10^{-6} [kPa] distribution along the 0º/90º interface of the $[0^o/90^o]_s$ and $[90^o/0^o]_s$ laminates under uniform axial strain, considering different mesh densities compared to analytical solution [2]

3.3. Distribution of the interlaminar normal stress σ_z

In Figure 4, the distribution of σ_z through the width of the plate with $[0^o/90^o]_s$ stacking sequence is shown. Results from different models in Abaqus are compared with analytical solution [2], for the interface at $z = h_k$. In the middle of the plate, the stress is close to zero, while the stress values are greatest close to the free edge with the maximum being reached exactly at the free edge. For the $[0^o/90^o]_s$ laminate, mesh refinement leads to the increase of the σ_z along the free edge. As in previous case, the C3D10 finite element provided results that are significantly more similar with the analytical ones.

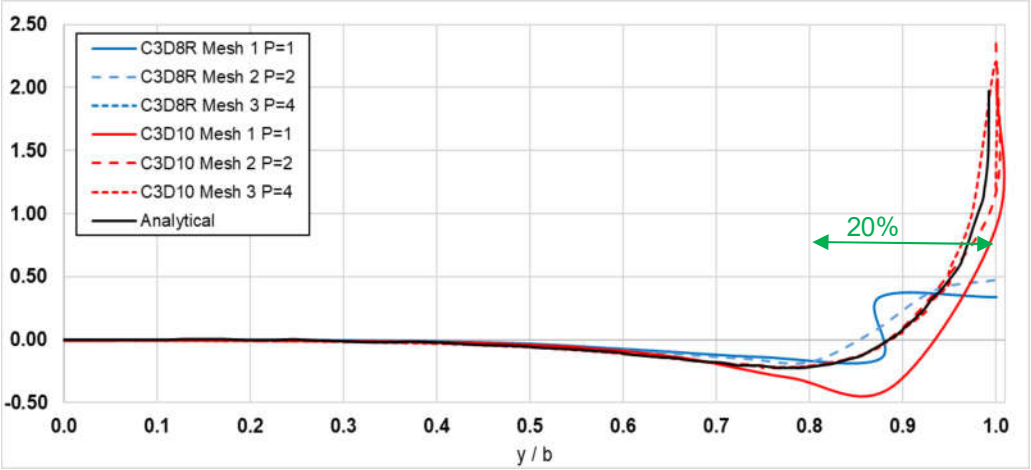

Figure 4. Dimensionless interlaminar normal stress (σ_z / ε_0)×10^{-6} [kPa] distribution along the 0º/90º interface ($z = h_k$) of the $[0^o/90^o]_s$ laminate under uniform axial strain, considering different mesh densities compared to analytical solution [2]

In Figure 5, the distribution of σ_z through the width of the plate with $[90^o/0^o]_s$ stacking sequence is displayed, for $z = h_k$ interface. The stress is close to zero in the middle of the plate width, gradually increasing towards the edges and sharply rising in the last 20% of the half-width, where it also changes the sign from positive to negative. This trend is also observed in the analytical solution.

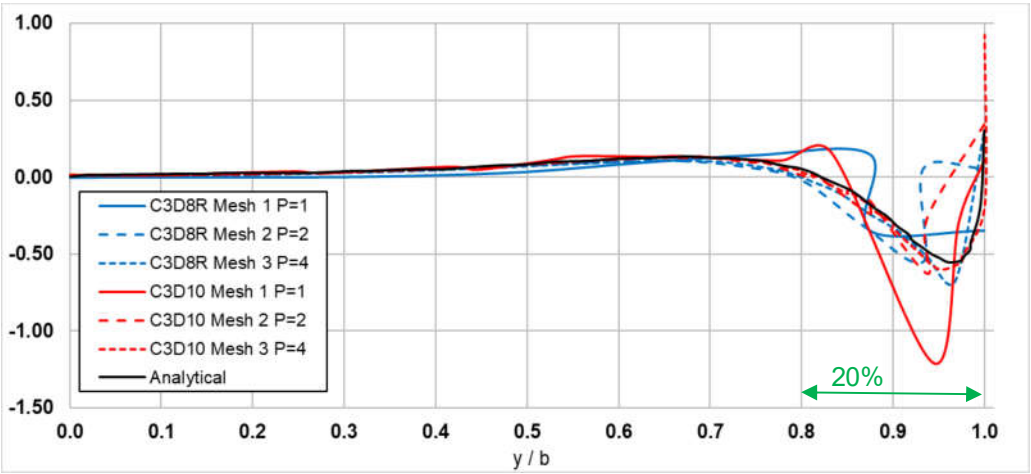

Figure 5. Dimensionless interlaminar normal stress (σ_z / ε_0)×10^{-6} [kPa] distribution along the 90º/0º interface ($z = h_k$) of the $[90^o/0^o]_s$ laminate under uniform axial strain, considering different mesh densities compared with analytical solution [2]

3.4. Distribution of σ_z through the plate thickness

Figure 6 shows the distribution of interlaminar normal stress σ_z through the thickness of the plate with [0°/90°/0°/90°] cross-ply stacking sequence. The results are obtained by using the C3D8R finite element and considering different mesh densities (P=2 and P=4). The results show that σ_z reaches its peak values at the interfaces of two layers with different fiber orientations. It is also shown that the used meshes greatly underestimate the maximum values of σ_z stress when compared against the analytical solution. This means that mesh refinement should be adopted at least in the zones covering ~ 20% of the plate's half-width along the free edges (see Figures 4-5), to accurately predict the extreme values of σ_z which may cause delamination.

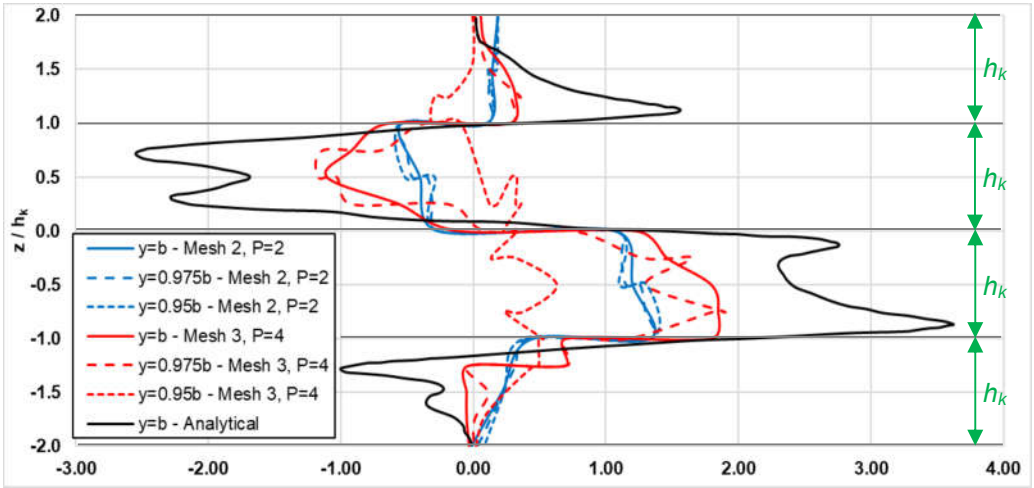

Figure 6. Dimensionless interlaminar normal stress (σ_z / ε_0)×10^{-6} [kPa] through the thickness in [0°/90°/0°/90°] laminate under uniform axial strain, considering different mesh densities compared to analytical solution [2]

3.5. Parametric study

As a benchmark study, a parametric anaysis on the influence of the plate (layer) thickness has been conducted. For this purpose, both C3D8R and C3D10 elements have been used. A 4-layers rectangular laminated composite plate with dimensions $10h \times 4h \times 4h_k$ has been analyzed (see Figure 2), where h_k is the layer thickness. The adopted material properties are the same as in the previous analyses, while only the stacking sequence $[0°/90°]_s$ has been considered. Four different plate thicknesses have been analyzed: $0.75h$, h, $1.25h$ and $1.75h$. For the through-the-thickness interpolation, two finite elements per layer have been adopted (P=2). For the in-plane discretization, the same element size has been adopted ($h_k/2$).

Interlaminar shear stress is near zero in the middle and increases toward the free edge where it reaches its maximum values. In the zone of around 70% of the plate's half-width, the element type selection does not play the important role because the obtained stress values are nearly the same (Figure 7). In the last 30% of the plate's half-width, the differences occur (see gray dots in Figure 7). For all considered plate thicknesses, C3D10 element provided slightly higher values of the interlaminar shear stress (red lines in Figure 7). For the C3D8R element, all selected plate thicknesses resulted in almost the same maximum value of the dimensionless interlaminar shear stress τ_{yz}.

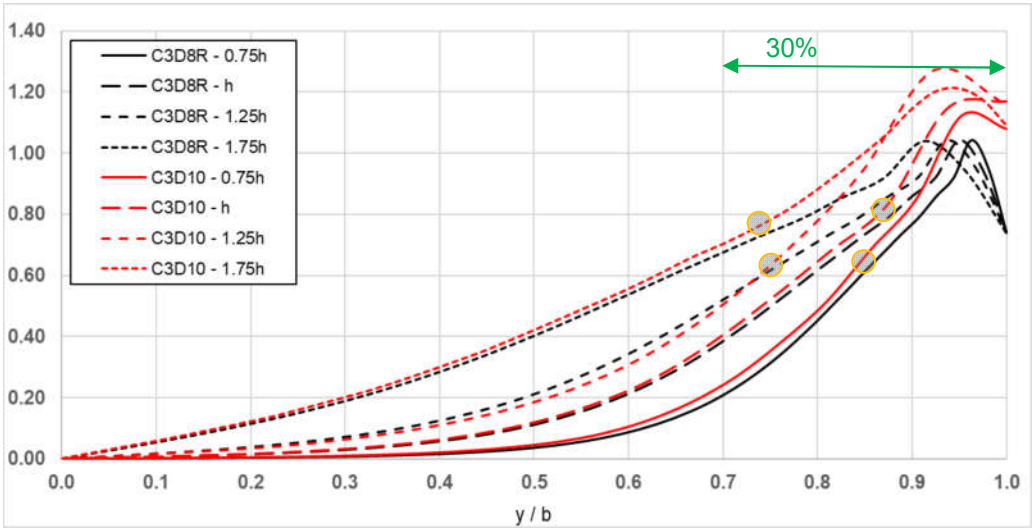

Figure 7. Dimensionless interlaminar shear stress (τ_{yz} / ε_0)×10^{-6} [kPa] distribution along the 0º/90º interface of the [0º/90º]$_s$ laminates under uniform axial strain, considering different plate thicknesses and different finite elements. Gray dots denote the points where higher differences in results from selected elements start to occur.

4. CONCLUSIONS

In the paper, two solid finite element types in Abaqus software have been used to evaluate the interlaminar shear and normal stress state near the free edges of a layered composite, under uniform axial extension. The distributions are analyzed through the width and through the thickness of a layered composite, considering different stacking sequences. Finally, a parametric study is performed to investigate the influence of layer thickness on the through-the-width distribution of the interlaminar shear stress τ_{yz}. The obtained results are compared against the analytical solution, proving the high accuracy of applied numerical models.

The distribution of τ_{yz} through the width of the plate, at layer interface, expectedly predicted the near-zero values in the middle and increase of τ_{yz} toward the free edge where it reaches its maximum values. The C3D10 elements showed better accuracy against the C3D8R in predicting both the position and the value of the maximum stress.

The analysis showed that in the middle of the plate, interlaminar normal stress σ_z is close to zero, with the greatest values close to the free edge and the maximum being reached exactly at the free edge. Mesh refinement led to the increase of the σ_z along the free edge. Again, C3D10 provided better agreement with the analytical results. For [90º/0º]$_s$ stacking sequence, σ_z is also close to zero in the middle of the plate widthe, increases towards the edges and sharply rises and changes sign in the last 20% of the half-width (also observed in the analytical solution). For all above scenarios, mesh refinement led to the convergence of results to analytical solution, as expected. The distribution of interlaminar normal stress σ_z through the thickness shows that σ_z reaches its peak values at the interfaces of two layers with different fiber orientations. However, the used meshes greatly underestimate the maximum values of σ_z when compared against the analytical solution.

The benchmark study on the influence of the plate thickness on the interlaminar shear stress distribution, showed that τ_{yz} is near zero in the middle and increases toward the free

edge where it reaches its maximum values. In the zone of around 70% of the plate's half-width, the element type selection does not significantly influences the results. In the remaining 30%, the differences occur. For all considered plate thicknesses, C3D10 element provided slightly higher values of the interlaminar shear stress when compared against C3D8R.

Future research will include the derivation of free-edge stresses using the original software based on the LWT, under complex load scenarios, such as bending and torsion.

ACKNOWLEDGMENTS

The financial support of the Ministry of Education, Science and Technological Development of the Republic of Serbia, through the project 200092, is acknowledged.

REFERENCES

[1] Reddy Junuthula Narasimha: **Mechanics of laminated composite plates and shells: theory and analysis**. *CRC Press*, Boca Raton, Florida, 2004.

[2] Tahani Masoud, Nosier Asghar: **Free edge stress analysis of general cross-ply composite laminates under extension and thermal loading**. *Composite Structures*, Vol. 60, No. 1, 91-103, 2003, https://doi.org/10.1016/S0263-8223(02)00290-8.

[3] Riepl Christoph: **FEM-Modeling of Composite Laminates considering Free Edge Effects**, Diploma Thesis, TU Wien, 2023.

[4] Pipes Byron, Pagano Nicholas J: **Interlaminar Stresses in Composite Laminates Under Uniform Axial Extension**. *Journal of Composite Materials*, Vol. 4, No. 4, 538-548, 1970, https://doi.org/10.1177/002199837000400409.

[5] Mittelstedt Christian, Becker Wilfried: **Interlaminar stress concentrations in layered structures: part I – a selective literature survey on the free edge effect since 1967**. *Journal of Composite Materials*, Vol. 38, No. 12, 1037–1062, 2004, https://doi.org/10.1177/0021998304040566.

[6] D'Ottavio, Michele, Vidal Philippe, Valot Emmanuel, Polit Olivier: **Assessment of plate theories for free-edge effects**. *Composites Part B: Engineering*, Vol. 48, 111-121, 2013, https://doi.org/10.1016/j.compositesb.2012.12.007.

[7] Becker Wilfried: **Closed-form solution for the free-edge effect in cross-ply laminates**. *Composite Structures*, Vol. 26, No. 1, 39–45, 1993, https://doi.org/10.1016/0263-8223(93)90042-O.

[8] Nosier Asghar, Bahrami Arash: **Free-edge stresses in antisymmetric angle-ply laminates in extension and torsion**. *International Journal of Solids and Structures*, Vol. 43, No. 22-23, 6800–6816, 2006, https://doi.org/10.1016/j.ijsolstr.2006.02.006.

[9] Nosier Asghar, Maleki M: **Free-edge stresses in general composite laminates**, *International Journal of Mechanical Sciences*, Vol. 50, No. 10, 1435–1447, 2008, https://doi.org/10.1016/j.ijmecsci.2008.09.002.

[10] Wang ASD, Crossman Frank W: **Some new results on edge effect in symmetric composite laminates**. *Journal of Composite Materials*, Vol. 11, No. 1, 1977, https://doi.org/10.1177/002199837701100110.

[11] ABAQUS User Manual 6.9. DS SIMULIA Corp., Providence, Rhode Island, USA, 2009.

[12] Dhondt Guido: **The Finite Element Method for Three-Dimensional Thermomechanical Applications**. Wiley, 2004.